International Journal of Engineering, Mathematical and Physical Sciences
ISSN: 2517-9934
Vol:5, No:4, 2011

Turbulent Mixing and its Effects on Thermal Fatigue in Nuclear Reactors

Eggertson, E.C. Kapulla, R, Fokken, J, Prasser, H.M.

***Abstract*—**The turbulent mixing of coolant streams of different temperature and density can cause severe temperature fluctuations in piping systems in nuclear reactors. In certain periodic contraction cycles these conditions lead to thermal fatigue. The resulting aging effect prompts investigation in how the mixing of flows over a sharp temperature/density interface evolves. To study the fundamental turbulent mixing phenomena in the presence of density gradients, isokinetic (shear-free) mixing experiments are performed in a square channel with Reynolds numbers ranging from 2'500 to 60'000. Sucrose is used to create the density difference. A Wire Mesh Sensor (WMS) is used to determine the concentration map of the flow in the cross section. The mean interface width as a function of velocity, density difference and distance from the mixing point are analyzed based on traditional methods chosen for the purposes of atmospheric/oceanic stratification analyses. A definition of the mixing layer thickness more appropriate to thermal fatigue and based on mixedness is devised. This definition shows that the thermal fatigue risk assessed using simple mixing layer growth can be misleading and why an approach that separates the effects of large scale (turbulent) and small scale (molecular) mixing is necessary.

***Keywords*—** Concentration measurements, Mixedness, Stably stratified turbulent isokinetic mixing layer, Wire mesh sensor

I. Introduction

CURRENTLY, many nuclear reactors worldwide are nearing or reaching their originally prescribed lifetime of approximately 40 years. In response, there are initiatives to address the main problems that limits this lifetime so that existing power plants can be safely kept in operation for longer (up to 60 years) and new power plants can be designed with a longer lifetime. One of these major problems is the phenomenon of thermal fatigue. The consequences of thermal fatigue in NPP's are exemplified by the failure of the residual heat removal loop in one of the reactors of the CIVAUX plant in France, an event investigated by Chapuliot with numerical analysis [1] and furthermore with the European THERFAT project [2]. Thermal fatigue can result in a failure of pipe walls in nuclear reactors and ultimately a loss of primary coolant. The fatigue arises from oscillating stresses in the wall that are coupled with the expansion and compression of the material due to oscillating temperatures. When two fluids streams of significantly different temperatures mix, before reaching homogeneity (or a level of good mixedness), they can expose a section of pipe wall to periodic fluctuations of temperature and potentially facilitate fatigue cracking.

When two streams with a strong temperature difference mix (such as in the residual heat removal cycle of a reactor) a strong density gradient also exists. The temperature differences can be as high as 160°C in normal operation which results in a density difference ($\Delta\rho$) of appr. 10%. Understanding how density interfaces affect the mixing of coolant streams is integral to predicting areas susceptible to thermal fatigue [3].Experiments discussed in this paper are performed on the GEMIX (**Ge**neral **Mi**xing E**x**periment) facility at the Paul Scherrer Institut in Villigen, Switzerland. GEMIX focuses on the basic mechanisms that promote or define mixing over a density interface. Concentrations are measured with Laser Induced Fluorescence (LIF) and a Wire Mesh Sensor (WMS). Velocity measurements are taken with Particle Image Velocimetry and although out of the scope of this paper, can be seen in work by Kapulla and Fokken [4], [5]. Similar experiments have been performed in T-junction geometries on the topic of thermal fatigue [2], [6] but GEMIX uses a generic square channel and isokinetic (shear-free) flow to achieve fundamental flow that is free from the effects of complicated geometry.GEMIX experiments are shear-free, which describes systems where the velocity gradient is close to zero, such as static stratifications or two flows with identical velocity (isokinetic). The energy necessary for mixing to occur in shear-free interfaces comes from the turbulence in the flowing streams and is proportional to the RMS of the crosswise velocity. The pioneers of research on stably stratified quiescent mixing was initiated by Rouse & Dodu [7] and brought to light by Turner [8], [9]. His work with the Richardson number and its relation to entrainment rates and mixing phenomenon sparked 20 years of constant research in static, grid-stirred, shear-free, turbulent mixing in a transient state, all of which is compiled in the exhaustive chronicle by Fernando [10].Steady state co-flow mixing is not as widely studied and research with water is limited to the saline-stratified experiments of Huq and Britter [11], [12] and a series of works under Van Atta in a number of test sections, but mostly limited to modeling of turbulence [13]. An interesting addition by Barrett and Van Atta is a transient experiment where a grid is towed through quiescent stratified water [14]. The tank is towed up to 50 times through the fluid allowing for turbulence to fully decay between tows so the

E. C. Eggertson is with the Schulich School of Engineering, University of Calgary, Calgary, AB Canada on internship with the Paul Scherrer Institut, Villigen, Switzerland; (phone: +41-77-481-2226; e-mail: eceggert@ucalgary.ca).

R. Kapulla is with the Paul Scherrer Institut, Villigen Switzerland; (e-mail: ralf.kapulla@psi.ch).

J. Fokken is with Axpo AG, Baden, Switzerland completing his PhD with the Paul Scherrer Institut; (e-mail: juerren.fokken@psi.ch).

H.M. Prasser is a professor at The Swiss Federal Institute of Technology (ETH) in Zurich.

static profile can be fully measured. The results are comparable to the expansion of a mixing layer in a steady state experiment, but without the effects of grid-generated turbulence decay in the flow direction. Less similar in nature but still relevant work in a heat-stratified wind tunnel by Jayesh and Warhaft [15] will also be useful for stratified growth law comparison. GEMIX is similar to [11]-[13], [15] as a forced, open-loop system in steady state, but differs in motive. The aforementioned three authors' experiments were mostly designed to analyze climate phenomena on an atmospheric scale. The scale difference between atmospheric and reactor flow leads to disparities in the design between GEMIX and other experiments, including GEMIX's comparatively small side length.One of the parameter of most interest is the height of the mixing layer, defined with multiple definitions. Kweon [3] demonstrates that the boundary layer thickness, defined as the transient temperature region, is nonlinearly and inversely proportional to the peak stress intensity, a measure of thermal fatigue crack propagation. It is shown that the definition of the thickness of the mixing layer can have profoundly different relationships to thermal fatigue and that traditional measures of the thickness are not wholly appropriate for investigations. Furthermore, the mixing layer height from WMS results will be judged as a function of three parameters: velocity (Re), distance from splitter plate tip (x_{WMS}) and density difference ($\Delta\rho$).

II. Experimental Setup

The components of the test section consist of the inlet, measurement and outlet sections. All components are made of acrylic glass except for the stainless steel splitter plate tip, which separates the two streams in the inlet section. The splitter plate gradually decreases in thickness before tapering to a tip, after which the streams are free to mix in a 50x50mm^2 square mixing section. Before the splitter plate tip, both streams pass through honeycombs and grids to condition the flow. The combined cross-sectional area of both streams is kept constant throughout the process. The measurement section (seen in fig. 1) extends 50-550 mm from the splitter plate tip. After a length of straight channel to limit backwards effects of the outlet channel, the flow is split again into two streams which are led over a weir that maintains constant back pressure in the channel. The flow is split to prevent the lighter fluid from 'climbing' over the denser fluid in the weir section, causing the denser fluid to accumulate at the base of the weir and create an uneven backwards or upstream effect.

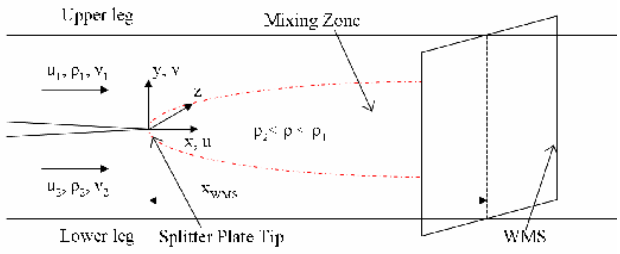

Fig. 1 Principal Sketch of GEMIX-Facility primary components

The channel is fed by two 2000 L tanks. One contains tap water and the other contains either pure de-ionized (DI) water or a solution of sucrose in DI water. The mass-fraction of sucrose in conjunction with temperature can be altered to set precise density differences between the streams while (in normal conditions) keeping the viscosity of the two streams similar. The isoviscosity prevents differences in the Re between streams that would affect symmetry. The streams are set at equal velocities and mix in a shear-free manner so that $u_1 = u_2 = u_0$, in a range from 0.05 - 1.2 m/s. In the measurement section, this translates to a range of Reynolds numbers between 2'500 - 60'000. The different sucrose solutions (in DI water) used to achieve certain density differences while keeping isoviscosity between streams are outlined in Table I.

TABLE I
Sucrose Solution Parameters

$\Delta\rho$	ρ_{tap} (g/L)	ρ_{DI} (g/L)	Sucrose Mass-%	T_{DI} (°C)
0%	998	998	0	20.0
1%	998	1008	2.71	22.5
3%	998	1028	8.20	29.0
5%	998	1048	13.80	37.2
10%	998	1098	28.46	65.7*

Parameters of the sucrose solutions that give the desired density differences of 0-10% are given. Values are based on $T_{tap} = 20°C$ but are adjusted if $T_{tap} \neq 20°C$. The solution for the $\Delta\rho = 10\%$ can not be heated past 50°C, but using a cooler solution has little effect on viscosity [16]

III. Wire Mesh Sensors (WMS)

The WMS is a developing technique that replaces a conductance probe by measuring local conductance over the entire cross section of the duct simultaneously with minimal solidity (10%). Most commonly, the difference in conductance between phases is used to map multiphase flow with the WMS, but by using conductive tap water and non-conductive DI-solution in each stream we can obtain a similar conductance map for single phase flow.

The WMS used in the GEMIX facility consists of two perpendicular arrays of 48 wires of diameter 0.05 mm that are spaced 0.5 mm from each other. The result is a matrix in the cross section of 48x48 measurement nodes. The first array consists of transmitting wires. Pairs of wires, one from each array are activated, with the transmitting wire exciting the receiving wire. The magnitude of the signal is proportional to the conductance of the fluid at the given node. The WMS covers the entire cross section of 50x50 mm^2 spaced equidistantly, so achieves a resolution of 1.08 mm. A sampling frequency of 2500 Hz is used at a standard measurement length of 60 seconds for each run to yield 150'000 conductance maps, or frames. A more detailed description of the WMS is outlined by Prasser [17].

The conductance can be converted into a non dimensional calibrated transport or "mixing scalar" as shown in the following equation:

$$\Theta = \frac{C - C_{DI}}{C_{tap} - C_{DI}} \quad (1)$$

Where C is the instantaneous conductance in arbitrary units. The values of C_{tap} and C_{DI} are obtained from calibration runs performed at the beginning of each set of experiments. In these measurements, the channel is flooded with only DI or tap water to achieve the bounds of possible conductance readings. The actual experiment reading will be normalized between the bounds and the resulting mixing scalar between 0 and 1 will show how well the fluid at that given node is represented by tap or DI water. The fluid at θ = 1 is pure tap water, at θ = 0 is pure DI water.

The three manipulated parameters of density difference, velocity and downstream distance are represented by values outlined in table II. The values are combined in every possibly combination to maximize the amount of data available.

TABLE II
FLOW PARAMETERS

Δρ (%)	u (m/s)	x_{WMS} (mm)
0%	0.2	50
1%	0.4	150
3%	0.6	250
5%	0.8	350
10%		450
		550

Every combination of these three parameters is tested. Additional velocities including laminar cases (0.05, 0.1, 0.15) and faster cases (1.0, 1.2) are also performed, but not necessarily for every instance of Δρ and x_{WMS}.

IV. RESULTS

A. Concentration Maps

Concentration maps are 48x48 matrices of data in the cross section where each element represents a node of the WMS. Fig. 2 displays maps for the mean ($\overline{\theta}$) and standard deviation (θ_{RMS}) of the mixing scalar. The first map (a) serves as a reference case and each of the other maps (b, c, d) have one parameter adjusted. These are shown as a general overview of the possible stable flows in GEMIX. Apparent in all cases is the formation of a mixing layer, a zone where the fluctuations of the mixing scalar are highest. The width of the interface is of utmost importance, and variance in the size can be seen in the sample images. The inversion of colour in fig. 2 (d) is due to an inversion of streams. The unstratified case actually has a Δρ < 0.05% where the tap water is naturally denser and therefore on the bottom. This difference is on the same scale as the precision of density readings from our Coriolis flow meters. Stratified cases always have the dense sugar solution in the DI water and therefore the DI is on the bottom.

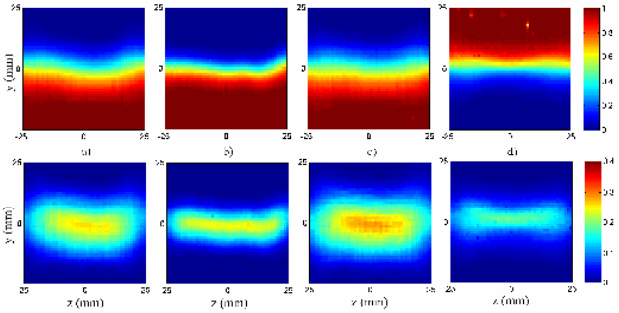

Fig. 2 Mean (upper) and RMS (lower) maps where a) u = 0.8 m/s, x_{WMS} = 550 mm and Δρ = 0%. Experiments b, c and d deviate from a) by one parameter: b) shows x_{WMS} = 250 mm, c) shows u = 0.4 m/s, and d) shows Δρ = 5%.

B. Profiles

The WMS and LIF show analogous and comparable data, but in different planes. To increase the lines of intersection between the methods, we change the position of the WMS along the length of the channel. The LIF data runs from x = 50 – 500 mm. The position of the WMS (x_{WMS}) is installed at intervals of 100 mm from 50 – 550 mm to give five lines of intersection as seen in fig. 3. Viewing raw images can reveal the shape and size of turbulent mixing elements at a given position but need further processing to give quantitative information. Further information on the use of LIF in GEMIX is covered by Fokken [18], [19].

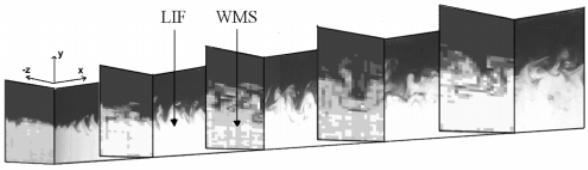

Fig. 3 The different planes of the WMS and LIF data and how they intersect are shown

Vertical profiles are extracted from the concentration maps for both LIF and WMS at the lines of intersection. The profiles are expressed in mean ($\overline{\theta}$) and RMS (θ_{RMS}) values of the mixing scalar. The profiles can be fit well with (2) for the $\overline{\theta}$ profile and (3) for the θ_{RMS} profile.

$$\overline{C}_{(y)} = \overline{C}_m - \frac{\Delta\overline{C}}{2} \cdot erf\left(\frac{y - y_{chr}}{\delta_h / 2}\right) \quad (2)$$

$$\overline{C}_{rms(y)} = \overline{C}_{mr} - \Delta\overline{C}_{rms} \cdot \exp\left[-\frac{(y - y_{chr})^2}{\delta_{hr}^2 / 2}\right] \quad (3)$$

The parameters have physical meanings that can be seen in fig. 4. The $\delta_{h/hr}$ parameter is of particular interest in the analysis, symbolizing the thickness of the mixing layer. The hyperbolic tangent function (tanh) is used in much of the early literature [8] to represent a density profile. However, it is evident that $\delta_{hr} \neq \delta_{tanh}$. It is shown that the error function, the

integral of the Gaussian function provides a better fit experimentally [11] and theoretically [20].

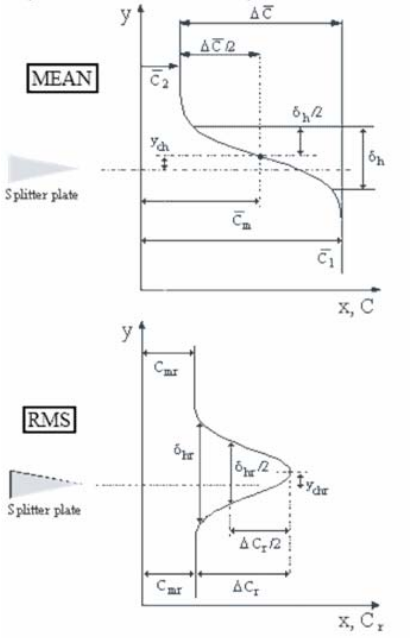

Fig. 4 Physical representations of the fit equation parameters. The error function above fits to a mean profile The Gaussian function on the right fits to an RMS profile

C. WMS Trends

The mixing layer thicknesses (δ_{hr} or δ_h) grow with x according to a power law where the relation is linear in the logarithmic plane. The power law changes little with velocity (for Re > 20000) and the power laws are averaged over these velocities to reflect this. There is a difference in magnitude between δ_{hr} and δ_h but the growth is fairly constant. Huq and Britter achieve a value of n = ½ [11] but our data in fig. 5, suggests closer to n = ⅔ when related as

$$\delta \propto x^n . \quad (4)$$

The growth law is known to be different for the stratified cases due most notably to turbulence decay [13] and therefore mixing layer contraction as demonstrated by Huq [12]. Further experimentation is necessary to gather the required data to formulate these growth laws.

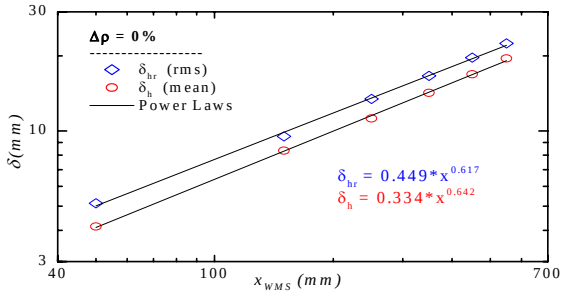

Fig. 5 The mixing layer thickness as a function of distance from the splitter plate can be considered to follow a power law. Here, data from the mean and RMS fits are shown to vary slightly, but have overall similar power laws. Δρ = 0%.

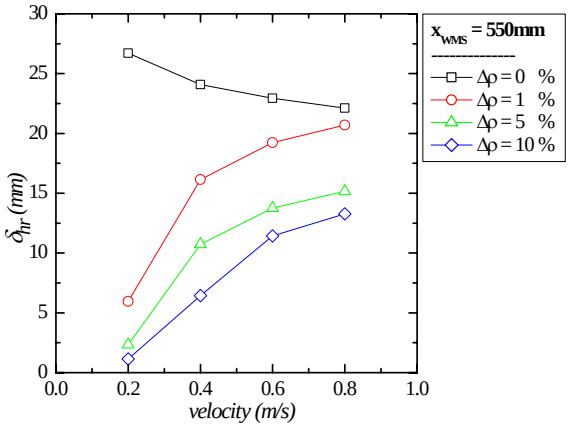

Fig. 6 The thickness of the interface as a function of velocity is shown for four different values of Δρ. x_{WMS} = 550 mm

Cases where x_{WMS} = 550 mm and Δρ = 0%, 1%, 5%, 10% are used to show the evolution of δ as a function of velocity. The results are shown in fig. 6. Firstly, it is shown that the mixing layer thickness decreases as Δρ increases for all velocities. It can also be seen that for the stratified cases, when the velocity is increased the mixing layer widens. For the unstratified case, we see the opposite, where higher velocity cases have a thinner mixing layer. This counter intuitive phenomenon is the impetus for the investigation in the remainder of this paper.

V. Discussion

A. Entrainment Power Law

The most widely used universal law between the size of the mixing layer based on downstream distance, density difference and bulk velocity is power law of the entrainment rate – Richardson number relation. The power law where $E \propto Ri^n$ was established by Turner [8], [9]. The entrainment rate represents the growth of the mixing layer thickness with time. This relation is important in transient experiments where concentration can only be measured at one location per experiment. A thickness, or rate of thickness growth, can then be assumed from the location of the probe and the measured mixing scalar assuming a tanh profile.

Previous steady state experiments all use traversing probes to measure mean density profiles [11]-[13], [15]. With this method, instantaneous profiles can not be measured and measurements at different locations rely on a high degree and steadiness. Huq [11] outlines the shortcomings of representing the stratification with a mean profile:

"*While the ultimate measure of mixing is the attainment of homogeneity at the molecular level, in turbulent flows, the mean density, or concentration profile, tells little about the degree of molecular mixing… Accordingly, when turbulence is present in fluid flows, the stirring of the fluid and the final process of molecular mixing should be examined*

individually… [but] they are not easily distinguishable experimentally."

The traditional definition of mixing layer thickness based on the mean profile, δ_h, has an inherent flaw most notable in the analysis of risk for thermal fatigue. When quantifying the flow, δ_h is a simple physical parameter that can be used for limited comparison, but that can also mislead on the state of the interface. With the WMS, measurement of instantaneous profiles is possible. It can be shown that δ_h is larger than the mean of the thickness of the instantaneous profiles, δ_i, where coherent instantaneous profiles are available (only strongly stratified flow, as seen in fig. 7). This is due mainly to a wandering or wavy interface, where y_i, the instantaneous equivalent of y_{ch} (as defined in fig. 4), oscillates in the y-direction. This creates a large mixing layer but still exhibiting a thin interface between pure streams.

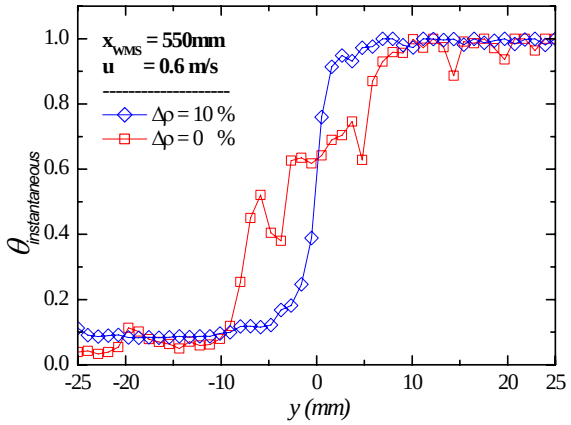

Fig. 7 Arbitrary instantaneous profiles from the WMS are irresolvable for unstratified flow due to eddy impingement, but are resolvable after significant turbulent decay in strongly stratified flows

B. Scale of Mixing

The important distinction is between large scale and small scale mixing henceforth referred to as macro- and micro-mixing. Macromixing occurs from turbulence and broadens the mixing layer but not the interface. Micromixing occurs from molecular diffusion and smears out the concentration gradients between the pure fluids, widening the interface. A problem exists in the resolution of the WMS, which is much larger than the Kolmogorov microscales. Mixing due to eddies of length scales smaller than the WMS resolution cannot be elucidated and is defined for our purposes as a product of micromixing. It is assumed that the majority of turbulent mixing occurs at length scales larger than the resolution of the WMS. Since both forms of mixing increase the mean mixing layer thickness, it can be said that mean thickness is a superposition of a hypothetical macromixing (+) thickness and micromixing (-) thickness:

$$\delta_h \propto \delta_+ + \delta_- \quad (5)$$

Relating these two hypothetical thicknesses to measurable physical thicknesses is the problem that Huq was alluding to in the previous passage. Simple definitions would be $\delta_- = \delta_i$ and $\delta_+ = \text{rms}(y_i)$. This technique would require instantaneous profiles to be fit with an error function for parameters to be extracted, but for most cases, the instantaneous profiles are irresolvable and don't give a reliable fit to the error function (fig. 7). Other parameters representative of δ_i and $\text{rms}(y_i)$ are necessary to separate micro and macromixing.

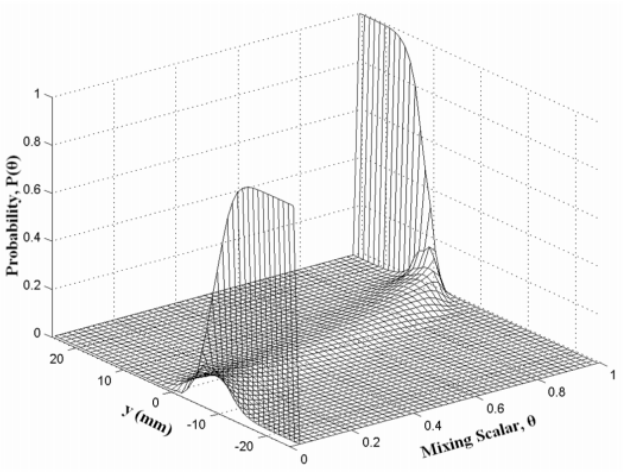

Fig. 8 Histograms of the concentrations at z = 0 mm for each value of y. Histograms are concatenated to produce a surface image. The degree of bimodality is used to represent mixedness

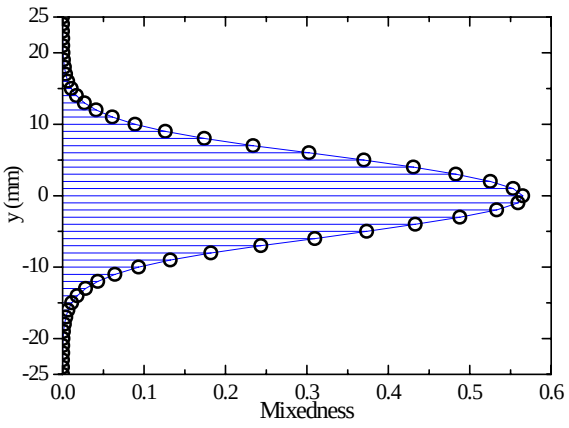

Fig. 9 A profile of the degrees of mixedness where highest mixedness is in the centre and pure streams at the extremes have a zero-mixedness

C. Mixedness

A degree of micromixing is presented by Koop and Browand [21] by the Mixedness parameter which has been adapted here from a density signal to θ signal:

$$M(z,y) = \frac{\int_0^T \left[(1-\theta(t))\cdot H(\theta(t)-\bar{\theta}) + \theta(t)\cdot H(\bar{\theta}-\theta(t))\right]dt}{\int_0^T \left[(1-\theta_b)\cdot H(\theta(t)-\bar{\theta}) + \theta_b \cdot H(\bar{\theta}-\theta(t))\right]dt} \quad (6)$$

Where $\bar{\theta}$ is the average mixing scalar at the node; H is the Heaviside function; T is the length of the signal and θ_b is the bulk mixing scalar (or θ for the homogeneously mixed fluid; $\theta_b = 0.5$ for the shear-free case). Mixedness represents the bimodality of the histogram of θ(t) or how long pure streams are present. A perfectly mixed solution where θ(t) = 0.5 gives M = 1 and an oscillation of two unmixed streams with an infinitely sharp interface and θ(t) = (0 U 1) (0 or 1) gives M = 0.

Using the profile at z = 0 mm, histograms are calculated for every value of y. These are concatenated and displayed in the surface plot in fig. 8. Every value of y gives a different value for M, the maximum of which exists at y_{ch} with minima at y = ±25 mm as seen in fig. 9. Furthermore, a new definition of thickness [21] can be derived from the mixedness profile from fig. 9 according to:

$$\delta_M = \tfrac{1}{2}\int_z M(y)dy\,. \quad (7)$$

The lack of data with resolvable instantaneous profile renders comparisons of δ_M and δ_i difficult. Using a virtual signal to represent WMS data with completely resolvable instantaneous profiles, fig. 10 shows that the correlation $\rho(\delta_i, \delta_M)$ is much higher than $\rho(\delta_i, \delta_h)$ or $\rho(\delta_i, \delta_{hr})$ and therefore that δ_M is a good representation of δ_i. An in situ comparison can be imposed on experiments with a strong ($\Delta\rho = 10\%$) stratification as turbulence decay occurs within the measurement section and at this point the instantaneous profiles are mostly resolvable. Barrett visually shows how turbulent decay affects the instantaneous density profile [13]. The in situ correlation $\rho(\delta_i,\delta_M) = 0.9984$ is high showing that δ_M is a good representation of δ_i, but $\rho(\delta_i, \delta_h) = 0.9977$ is not much lower. For this case, the extensive turbulence decay also leads to the fading of macromixing and causes $\delta_+ << \delta_-$ and thus $\delta_h \approx \delta_-$. It follows that δ_M as a tool to separate macro and micromixing is most useful when its accuracy can not be proven (when δ_i is irresolvable), but there should be enough proof of concept to extrapolate the relation $\delta_M \approx \delta_i \approx \delta_-$ for all cases.

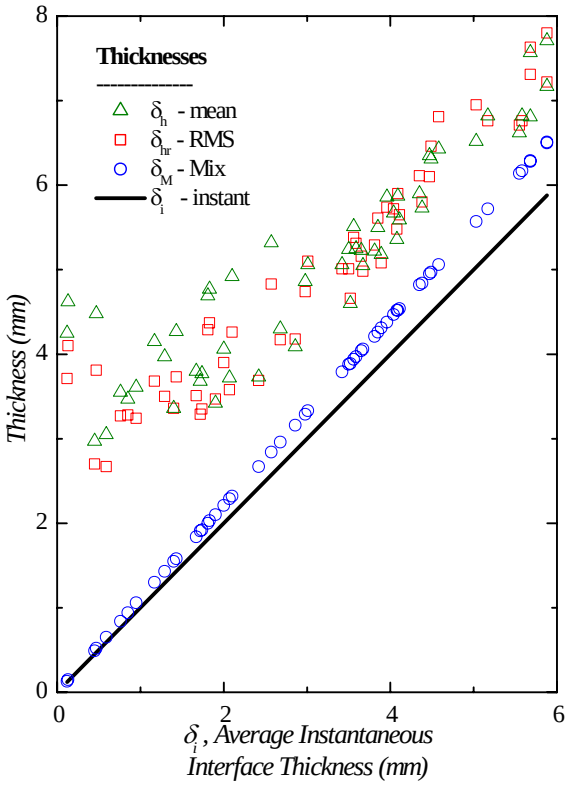

Fig. 10 Scatter plot show the correlation between δ_i and other thicknesses. $\rho(\delta_i, \delta_h) = 0.9066$, $\rho(\delta_i, \delta_{hr}) = 0.9454$, $\rho(\delta_i, \delta_M) = 0.9999$ for the analysis of a virtual signal shown here

The phenomena of turbulent decay results in the arrest of macromixing and decrease in δ_h with x. This decrease proves to be a problem with the entrainment power law, which only accounts for positive growth. Huq and Britter show the nonlinear power law for all stratified cases [11]. The solution has been to exclude data after the point of onset of mixing layer contraction from the power law fit [11], [22].

When the turbulence decays, the result is a flat interface that is the sole product of micromixing. This is the effect that produces resolvable instantaneous profiles. Although δ_h decreases, the micromixing is irreversible and δ_M should continue to grow at a similar rate. Growth laws based separately on δ_- and δ_+ could give a more universally applicable relation than the entrainment power law.

Further supporting the use of δ_M is the evidence of the profiles of the strongly stratified cases that are not represented well by Gaussian or error function fits as seen in fig. 11. The R^2 value for the error function fit of the mean profile of an unstratified case ($R^2 = 0.9998$) is about 10x closer to unity than a comparable $\Delta\rho = 10\%$ experiment ($R^2 = 0.9979$). The use of δ_M circumvents the use of parameters from a bad fit.

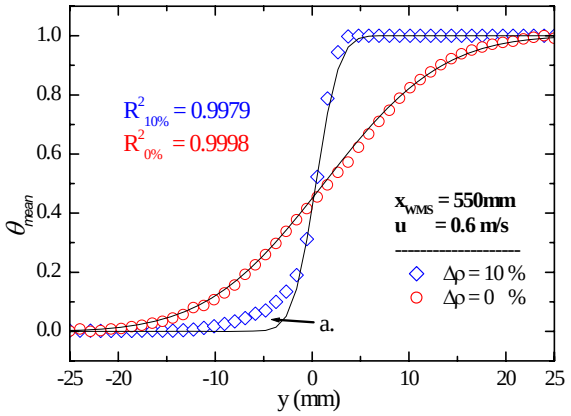

Fig. 11 Goodness of fit is represented for the Δρ = 0%, 10% cases. The goodness of fit based on the R^2 value for stratified cases are poorer due mainly to the phenomena seen at point a visible in all strongly stratified experiments

The effect of using δ_M instead of comparing different experiments can be seen in fig. 12 ($\delta_M = f(u)$) when compared to fig. 6 ($\delta_{hr} = f(u)$). Every level of stratification changes, but the most notable difference is in the trend for the unstratified case. δ_{hr} modeled u = 0.2 m/s as having a larger mixing layer than higher velocities, but δ_M shows that it also has the lowest level of micromixing and in this sense is not as "well-mixed".

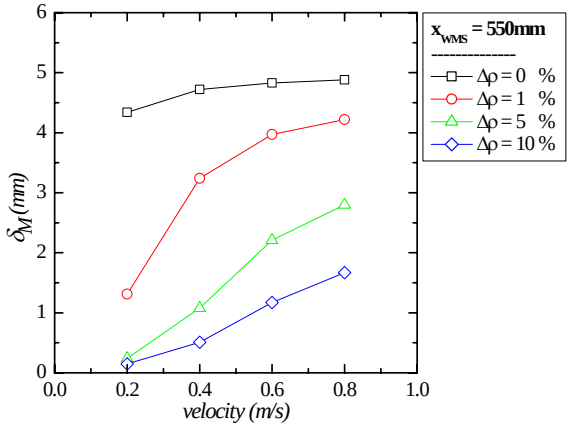

Fig. 12 The mixedness thickness δ_M is judged as a function of velocity. The differences with fig. 6 are notable

VI. Conclusion

Isokinetic mixing experiments stratified by sucrose are conducted in the GEMIX facility and measured using the Wire Mesh Sensor. The experiments are conducted at different velocities and density differences with the WMS installed at different distances from the splitter plate. The traditional measure for the extent of mixing in steady state stratified experiments has been the mean profile width, δ_h. It is shown that δ_h for the unstratified case grows with x according to the power law (3) mostly independent of velocity. More experimentation with different x_{WMS} is necessary to derive a growth law for the stratified cases from the. It is observed that stratification decreases δ_h for all Re and high Re increases δ_h for all non-zero stratifications. For the unstratified case, it is observed that δ_h decreases with Re.

This counter-intuitive observation prompted the creation of a variable that could describe the flow better and separate the effects of micromixing from macromixing, an important step in relating the flow back to thermal fatigue. The instantaneous thickness, δ_i, is considered to represent the total micromixing, but can not be directly measured due to irresolvable profiles. A definition of mixedness based on the bimodality of a signal is defined and when integrated over the centre profile as in (6), a new definition of thickness, δ_M, is derived. It is shown that this definition of thickness correlates to δ_i very well using virtual signals and strongly stratified experiments where instantaneous profiles are resolvable. Hence, δ_M can be used as quantification of the amount of micromixing.

When we analyze the effects of stratification and velocity on δ_M, we see mostly similar effects as before with the use of δ_h. The most important change is the inversion of the trend for δ(Re) for the unstratified case from being inversely proportional to being proportional to Re and resembling the trend of the stratified δ(Re).

The different levels of micro and macromixing affect thermal fatigue oppositely. A large amount of micromixing and thick interface decreases the risk whereas a large amount of macromixing or thermal striping increases the risk. It is important in accessing risk of thermal fatigue that both contributors be considered. A measure of the macromixing proportional to δ_+ and analogous to δ_M is desired to conclusively prove the superposition. Until this is defined, δ_M and δ_h are sufficient in giving an approximate ratio between micro and macromixing as well as the combined magnitude of both.

References

[1] S. Chapuliot, C. Gourdin, T. Payen, J.P. Magnaud, and A. Monavaon, "Hydro-thermal-mechanical analysis of thermal fatigue in a mixing tee," in *Nuclear Engineering and Design*, vol. 235, 2005, pp. 575-596.

[2] K.J. Metzner and U. Wilke, "European THERFAT project – Thermal fatigue evaluation of piping system tee-connections," in *Nuclear Engineering and Design*, vol. 235, 2004, pp. 473-484.

[3] H.D. Kweon, J.S. Kim, and K.Y. Lee, "Fatigue Design of nuclear class 1 piping considering thermal stratification," in *Nuclear Engineering and Design*, vol. 238, 2008, pp. 1265-1274.

[4] R. Kapulla, C. Dyck, M. Witte, J. Fokken, A. Leder, "Optical flow and cross correlation techniques for velocity field calculation," in *2009 Conf. Proc. Lasermethoden in der strömungsmesstechnik*, pp. 284-295.

[5] J. Fokken, R. Kapulla, S. Kuhn, C. Dyck, H.M. Prasser, "Stably stratified isokinetic turbulent mixing layers: Comparison of PIV-measurements and numerical calculation," in *2009 Conf. Proc. Lasermethoden in der strömungsmesstechnik*, pp. 296-303.

[6] C. Walker, M. Simiano, R. Zboray, and H.M. Prasser, "Investigations on mixing phenomena in single phase flow in a T-junction geometry," in *Nuclear Engineering and Design*, vol. 239, 2009, pp. 116-126.

[7] H. Rouse and J. Dodu, "Turbulent diffusion across a density discontinuity," in *Houille Blanche*, vol. 10, 1955, pp. 522-532.

[8] J.S. Turner, "The influence of molecular diffusivity on turbulent entrainment across a density interface," in *Journal of Fluid Mechanics*, vol. 33, 1968, pp. 639-656.

[9] J.S. Turner, "Buoyancy effects in fluids," *Cambridge: University Press*, 2nd ed., 1980, 368 pp.
[10] H.J.S. Fernando, "Turbulent mixing in stratified fluids," in Annual *Review of Fluid Mechanics*, vol. 23, 1991, pp. 455-493.
[11] P. Huq and R. Britter, "Mixing due to grid-generated turbulence of a two-layer scalar profile," in *Journal of Fluid Mechanics*, vol. 285, 1995, pp. 17-40.
[12] P. Huq and R. Britter, "Turbulence evolution and mixing in a two-layer stably stratified fluid," in *Journal of Fluid Mechanics*, vol. 285, 1995, pp. 41-67.
[13] E.C. Itsweire, K.N. Helland, and C.W. Van Atta, "Evolution of grid-generated turbulence in a stably stratified fluid," in *Journal of Fluid Mechanics*, vol. 162, 1986, pp. 299-338.
[14] T.K. Barrett and C.W. Van Atta, "Experiments on the inhibition of mixing in stably stratified decaying turbulence using LDA and LIF," in *Physics of Fluids*, vol. 3, 1991, pp. 1321-1332.
[15] Jayesh and Z. Warhaft, "Probability distribution, conditional dissipation, and transport of passive temperature fluctuations in grid generated turbulence," in *Physics of Fluids*, vol. 4, 1992, pp. 292-307.
[16] Z. Bubnik, P. Kadlec, D. Urban, M. Bruhns, "Sugar Technologists Manual," *Bartens pub co*. Berlin, 1995, pp. 125-170.
[17] H.M. Prasser, A. Böttger, and J. Zschau, "A new electrode-mesh tomograph for gas-liquid flows," in *Flow Measurement and Instrumentation*, vol. 9, 1998, pp. 111-119.
[18] J. Fokken, et al, "LIF-measurements and self similarity considerations in a stably stratified isokinetic turbulent mixing layer," in *2010 Conf. Proc. Lasermethoden in der strömungsmesstechnik*, pp. 12-19.
[19] J. Fokken, R. Kapulla, G. Galgani, O. Schib, H.M. Prasser, "Stably stratified isokinetic turbulent mixing layers: Investigation in a square flow channel," in *2010 Conf. Proc. International Youth Nuclear Congress*, pp. 120.1-120.9.
[20] H. Tenekes, J.L. Lumley, "A first course in turbulence," *MIT Press*, 1972, 300 pp.
[21] C.G. Koop and F.K. Browand, "Instability and turbulence in a stratified fluid with shear," in *Journal of Fluid Mechanics*, vol. 93, 1979, pp. 135-159.
[22] Xuequan E. and E.J. Hopfinger, "On mixing across an interface in stably stratified fluid," in *Journal of Fluid Mechanics*, vol. 166, 1986, pp. 227-244.